



HAL
open science

Analytical model for SiC based power converter optimization including EMC and thermal constraints

Gnimdu Dadanema, M. Delhommais, François Costa, Jean-Luc Schanen, Y. Avenas, Christian Vollaire

► **To cite this version:**

Gnimdu Dadanema, M. Delhommais, François Costa, Jean-Luc Schanen, Y. Avenas, et al.. Analytical model for SiC based power converter optimization including EMC and thermal constraints. 2017 International Symposium on Electromagnetic Compatibility (EMC EUROPE), Sep 2017, Angers, France. 10.1109/EMCEurope.2017.8094757 . hal-01736156

HAL Id: hal-01736156

<https://hal.science/hal-01736156>

Submitted on 16 Mar 2018

HAL is a multi-disciplinary open access archive for the deposit and dissemination of scientific research documents, whether they are published or not. The documents may come from teaching and research institutions in France or abroad, or from public or private research centers.

L'archive ouverte pluridisciplinaire **HAL**, est destinée au dépôt et à la diffusion de documents scientifiques de niveau recherche, publiés ou non, émanant des établissements d'enseignement et de recherche français ou étrangers, des laboratoires publics ou privés.

Analytical model for SiC based power converter optimization including EMC and thermal constraints

G. Dadanema¹, M. Delhommais², F. Costa⁴, J.L. Schanen², Y. Avenas², C. Vollaire³

¹ SATIE – ENS Paris Saclay, 61, Avenue du Président Wilson, 94230 Cachan, France

² G2ELab – Univ Grenoble Amps Cs 90624, 38031 Grenoble CEDEX1

³ AMPERE – Ecole Centrale de Lyon, 69134 Ecully, France

⁴ ESPE – Université Paris Est Créteil, 08 rue du général SARRAIL, 94000 Créteil, FRANCE

Abstract—A Model dedicated to EMI prediction in a DC-DC converter is presented in this paper. The model is analytical to be used by a deterministic optimization algorithm. This model not only predicts EMI but also thermal effects of the converter. Numerical and experimental validation of the model are performed regarding EMC aspects and perspectives for the final optimization purpose are presented.

Keywords—EMC ; analytical model ; optimization ; thermal; WBG semi-conductors

I. INTRODUCTION

Weight optimization is one of the most important issue that faced manufacturers nowadays. Moreover in transportation, weight is very critical because it greatly affects system efficiency and costs. To address this weight issue, multiple solutions are explored and the most promising is the use of wide band gap semi-conductors. Indeed, wide band gap semi-conductor such as Silicon carbide (SiC) or Gallium Nitride (GaN) allow an increase in operating frequency and temperature. Increasing the switching frequency of a power converter allow a reduction of the passives which accounts for a large share of the total weight of the converter. On the other side power losses increases with the switching frequency and consequently the heatsink volume is impacted. Though the conventional filter volume may benefit from the greater switching frequency, it's well known that EMC problems become important with high switching frequency and this impacts the EMC filter design. An optimization process is therefore inevitable to ensure a good design and a minimum weight of the power converter. The optimization process is very important but it efficiency is directly related to the model accuracy and complexity. Generally speaking, the more complex the model is the more accurate it will be. However, complex model can cause prohibitive simulation and optimization time. The developed model must overcome the trade-off relationship between complexity and accuracy.

In this paper, accurate SiC power MOSFET and Schottky Diode VHDL-AMS models are implemented and use in circuit simulator (Simplorer®), for the time domain switching behavior analysis of the DC-DC converter. Parasitic elements used in the simulation are extracted numerically by a finite element tool (ANSYS Q3D) using method of moment. These

parasitic elements and components models are completed with a load model and a bulk capacitor model for a complete and accurate time domain simulation which will serve as reference for the later simplified models. Part II presents the validation of these main models used for time domain simulation. This complex time domain simulation model is simplified in part III to serve as a study model for the synthesis of waveform analytical equations. The equations takes into account thermosensitive elements and are used to build equivalent voltage and current source that replace active components for a new time domain simulation. This last simulation with the equivalent sources results are compared to the first complex simulation result and measurement results for validation in part IV. We finally present how to use the analytical source model in the frequency domain, to build a complete analytical and accurate model for EMC prediction.

II. TIME DOMAIN SIMULATION OF THE DC-DC CONVERTER

The DC-DC converter is a simple 1 kW buck converter with 400 V input voltage and 0.5 duty cycle. A DO-160 5 μ H LISN (line impedance stabilization network) is used for EMC measurement. The complete equivalent schematic simulated is presented in *Fig. 1*. The DC link capacitor, the LISN and the load are measurement based models and the SiC power MOSFET and Schottky diode are physic based models. All the stray elements due to PCB (printed circuit board) are numerically extracted.

A. Active components models for analog simulation

The SiC power MOSFET modeling approach use in this paper is based on Hefner power MOSFET model [1]. A datasheet driven parameter extraction is used to define model parameters [2]. The final power MOSFET model integrates temperature scaling parameter that allow device performance evaluation over temperature. *Fig. 2* shows comparison between datasheet and a CREE MOSFET C2M0080120D output characteristics and capacitance.

The power Schottky diode model parameters extraction have been presented in [3] and *Fig. 3* shows statistic characteristics and capacitance of a CREE power Schottky diode C4D20120D data compare to model results.

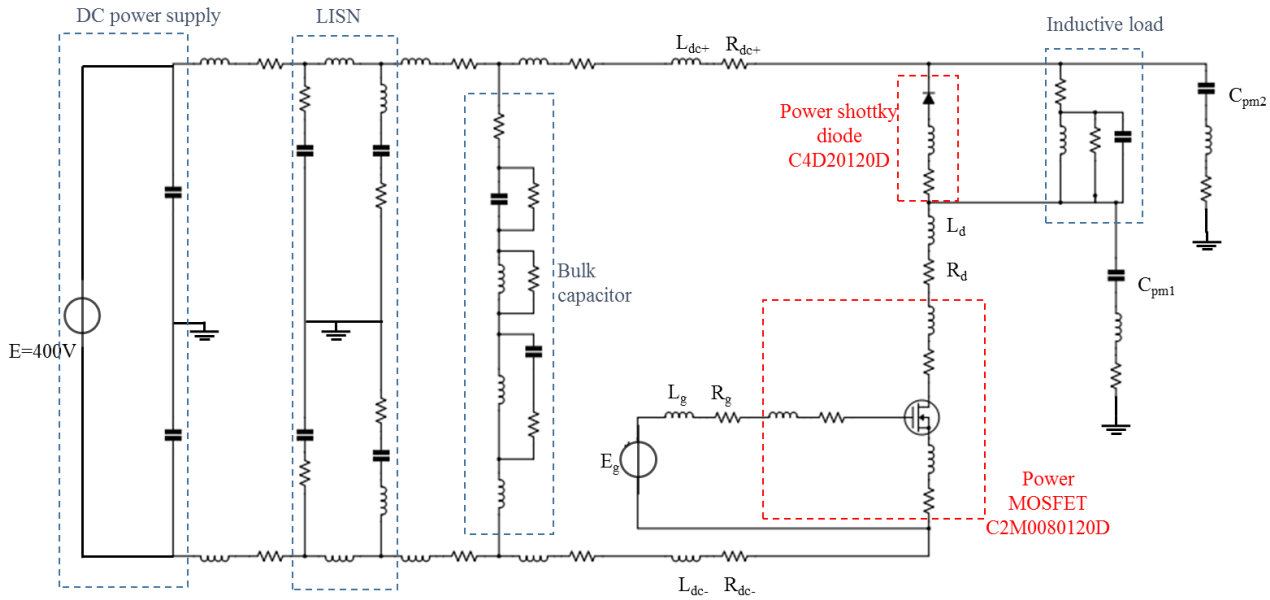


Fig. 1. Complete DC-DC converter simulation schematic
All these extracted parameters are used to elaborate VHDL-AMS component model for circuit simulation.

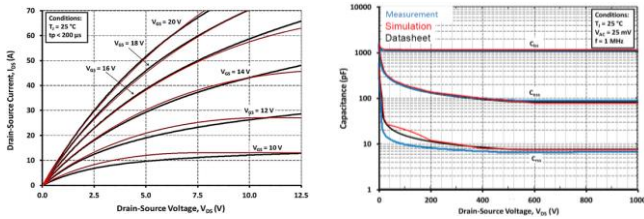


Fig. 2. Comparison between model (red) and datasheet. Left: Mosfet output characteristic. Right: Mosfet capacitance

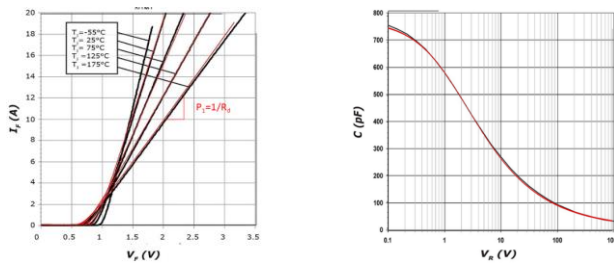


Fig. 3. Comparison between model (red) and datasheet. Left: Schottky diode forward characteristic. Right: Schottky diode capacitance

B. load modeling

The load used in the test bench consist of a 200 μH inductance in series with a 47 Ohms non inductive resistor. Measurements were performed to evaluate the stray capacitance between each element and the ground plane as they are important for the common mode study. The equivalent parallel resistance (EPR) and capacitance (EPC) of the inductance have been also measured to ensure a good representation of the load over a large frequency (up to 30 MHz) range. The final electrical model of the load is presented in Fig. 4

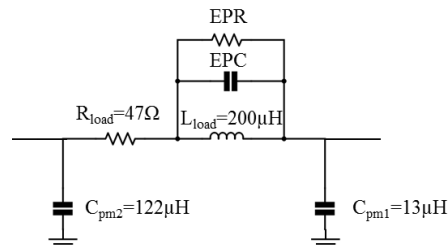


Fig. 4. Load electrical model

C. Input capacitance modeling

The bulk capacitance used in the test circuit is a 100 μF film capacitance. A behavioral model is used to fit capacitor impedance measurement data. Fig. 5 shows the final model values.

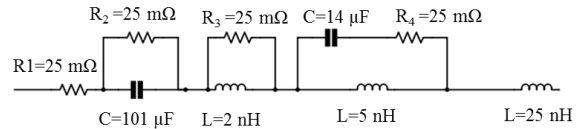


Fig. 5. Complete bulk capacitor behavioral model

D. LISN modeling

The LISN used in the test bench is compatible with the RTCA DO-160F [4]. The LISN element have been identify after measurement and the extracted elements and values are presented in Fig. 6.

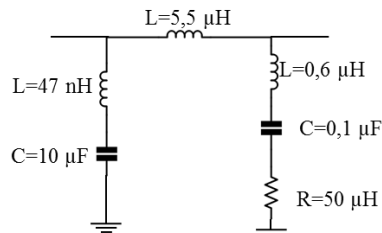


Fig. 6. LISN main electrical elements

E. Parasitic elements extraction

The PCB stray elements is very impactful in the switching behavior analysis of the commutation cell. There is two different approaches for the PCB modeling. The first one based on measurement is time consuming and cannot be applied in complex PCB design. The other approach is based on simulation and is more practical. This latter approach, is used in this work to extract parasitic elements of the PCB. The extracted stray PCB elements in this paper are obtained by ANSYS Q3D Extractor. In Q3D, The first step is to upload a 3D geometry of the PCB and next to define material properties dimensions, excitations (sources and sinks). After running the simulation parasitic elements are extracted with respect to defined calculation nodes (sources and sinks) as matrix and can be export as is, or user can manually define elements in the circuit simulator. In Ansys Q3D it's possible to export parasitic element matrix as a netlist to easily use it in a circuit simulator as Ansys Simplorer or Synopsys Saber.

For complex PCB design the use of the exported netlist is inevitable but for simple double layer PCB design like the one used for this paper we can manually define stray inductance, mutual and capacitor based on matrix analysis. Using this method we quickly define the equivalent electrical model of the PCB. Fig. 7 shows the main stray elements extracted from Ansys Q3D.

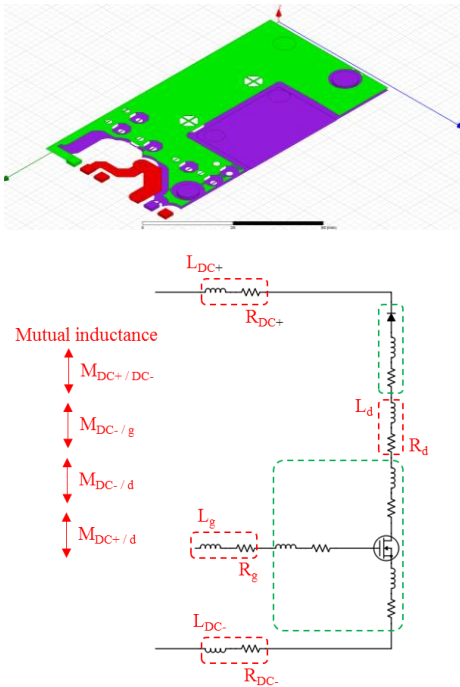


Fig. 7. Top : imported geometry in Ansys Q3D. bottom : stray elements in red and mutual inductance between all the inductances

III. ANALYTICAL WAVEFORM MODEL FOR EMI PREDICTION

Considering the previously modeled DC-DC converter, we simplify the schematic for analysis purpose. The important parasitic elements to take into account are the power loop equivalent resistance and the inductance that will impact the

current overshoot at the turn-on. The inductance L_s , can slow down the turn-on because the rising drain current create a voltage drop that slowed down the gate to source voltage rising. However, taking into account L_s complicates equation resolution, so we optimize the PCB design to minimize it and we neglected it in the analysis. The inductive load can be assimilated to a current source when solving the circuit equations and the capacitor to a voltage source. We finally reduced the complete simulation schematic of Fig. 1 to the simple analysis test circuit of Fig. 8.

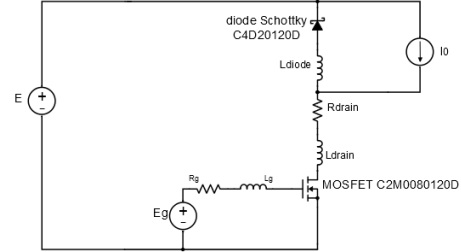


Fig. 8. Analytical model study circuit

Based on this simplified schematic, the switching period is decomposed in ten steps. For each step the procedure will be the same. We first identify the equivalent circuit associated to the switching step, we resolve the circuit equation to obtain current and voltage values. These successive current and voltage equations can be used to rebuild the switching waveform of the commutation cell in the time domain. With the waveform in time domain using a fast Fourier transform a spectrum is obtain for EMC analysis. On the other side, the equations integrates thermosensitive parameters such as the threshold voltage (V_{TH}), the transconductance (g_m) and the on-state resistance (R_{on}), that allows to rebuild a complete waveform for different working temperatures.

The MOSFET electrical model depends on the switching step, so we can have different values of MOSFET parasitic capacitance. In fact, the nonlinear behavior of MOSFET capacitance can be modeled in different way[5],[2] Propose to model them by power function but in our case it will add complexity to our equations and make them hard to solve analytically. Thus we will use a simpler methodology. Considering the representation of a nonlinear capacitance as shown on Fig. 9, we will define capacitance with subscript 1 as the capacitance value to be used when MOSFET is working in saturation region. Similarly, if the MOSFET is working in linear region we will define capacitance with subscript 2.

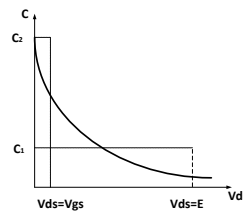
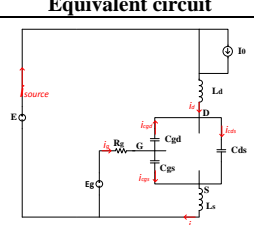
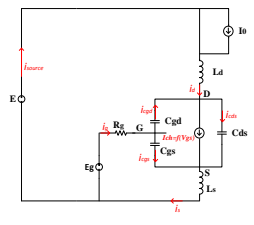
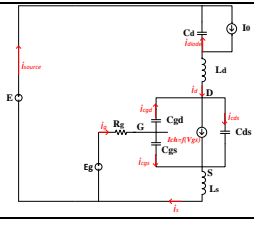
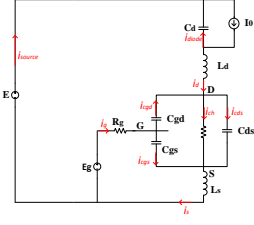


Fig. 9. Discrete capacitance value selection

TABLE I. CURRENT AND VOLTAGE EQUATIONS FOR DIFFERENT CIRCUIT CONFIGURATIONS

Equivalent circuit	Steps	V _{ds} (t), i _d (t)
	<i>t</i> ₀ - <i>t</i> ₁	$V_{ds} = E$ $i_d = 0$
	<i>t</i> ₉ - <i>t</i> ₁₀	$V_{ds} = (V_{dspic} - E)e^{\gamma t} \cos(\omega_0 t - \phi) + E$ $i_d = C_{oss1} \frac{dV_{ds}}{dt}$
	<i>t</i> ₁ - <i>t</i> ₂	$V_{ds} = E - (L_s + L_d) \frac{di_d}{dt}$ $i_d = g_m (V_{cc} - V_{th}) \left(1 + \frac{r_2}{r_1 - r_2} e^{\gamma(t-t_1)} + \frac{r_1}{r_2 - r_1} e^{\gamma(t-t_1)} \right)$
	<i>t</i> ₈ - <i>t</i> ₉	$V_{ds} = E - (L_s + L_d) \frac{di_d}{dt}$ $i_d = g_m (V_{cc} - V_{th}) \left(1 + \frac{r_2}{r_1 - r_2} e^{\gamma(t-t_1)} + \frac{r_1}{r_2 - r_1} e^{\gamma(t-t_1)} \right)$
	<i>t</i> ₂ - <i>t</i> ₃	$V_{ds} = - \frac{g_m (V_{cc} - v_{th}) - I_0}{g_m R_g C_{gd2} + C_{oss1} + C_d} (t - t_2) + E_1$
	<i>t</i> ₇ - <i>t</i> ₈	$i_{d_2} = I_0 e^{\gamma(t-t_2)} (\gamma \cos(\omega_0(t-t_2) - \phi) - \omega_0 \sin(\omega(t-t_2) - \phi))$
	<i>t</i> ₃ - <i>t</i> ₄	$V_{ds} = - \frac{g_m (V_{cc} - v_{th}) - I_0}{g R_g C_{gd2} + C_{oss2} + C_d} t + V_{gsd_0}$ $i_{d_2} = I_0 e^{\gamma t} (\gamma \cos(\omega_0 t - \phi) - \omega_0 \sin(\omega t - \phi))$
	<i>t</i> ₅ - <i>t</i> ₆	$V_{ds} = - \frac{g_m (V_{cc} - v_{th}) - I_0}{g R_g C_{gd2} + C_{oss2} + C_d} t + V_{gsd_0}$
	<i>t</i> ₆ - <i>t</i> ₇	$i_{d_2} = I_0 e^{\gamma t} (\gamma \cos(\omega_0 t - \phi) - \omega_0 \sin(\omega t - \phi))$

The expressions of the electrical quantities in the different working steps are summarized in table 1.

IV. RESULTS AND DISCUSSIONS

A. Results

Some high frequency Pearson® current probe are used with the LISN to extract common and differential mode current. The measured common and differential mode current are compare to the simulation result of the complete circuit of Fig. 1. Although simulating the circuit as is (with the active component complex model and all the stray elements) take a long time due to different time constant, it theoretically ensure consistent results for comparison with measurement. Fig. 10 shows the comparison results of the common mode current. We observe a relatively good agreement between simulations and measurement up to 30 MHz. This validates the time domain complete simulation circuit. We must now validate the simplified circuit that is used to define waveform equation. To

do so, the obtained waveform equations are used to define equivalent voltage and current sources and integrated to the simplify simulation circuit as illustrated by figure Fig. 12. The equivalent sources replace the active components of the commutation cell. This new circuit with the equivalent sources is simulated and the common mode current is compared to the measurement data in frequency domain after a fast Fourier transform in Fig. 12. The results show a good agreement between data up to 10 MHz. For the EMC filter design governed by the low side of the frequency range which is the final purpose of our model, these results are satisfactory. Discrepancies between data beyond 10 MHz can be explained by the simplification made for waveform equations synthesis and for some stray elements of the PCB. This last results validates the analytical voltage and current source representation for perturbations evaluation.

To validate the thermal behavior of the analytical waveform model simulation were performed for different temperatures.

Components working temperature can be define in the VHDL-AMS model of the component and waveform equations take

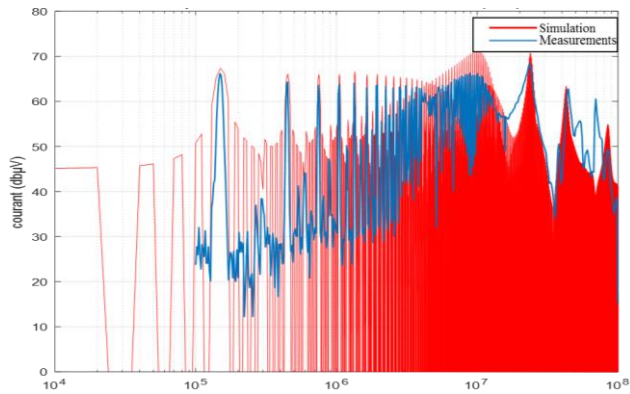


Fig. 10. Comparison between complete circuit simulation (red) and measured (blue) common mode spectra.

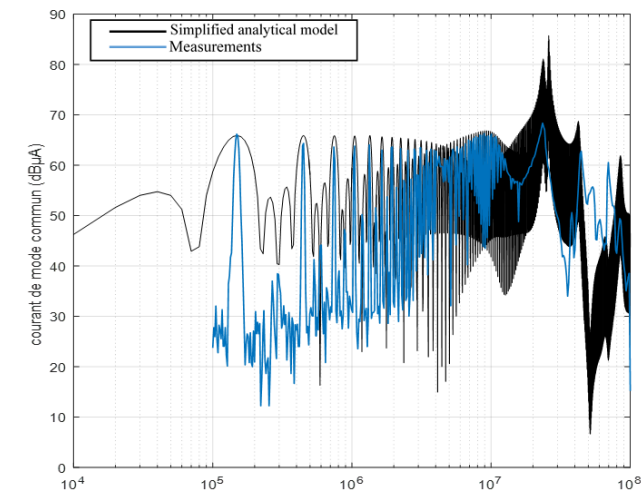


Fig. 11. Comparison between circuit with equivalent source (black) and measured common mode spectra

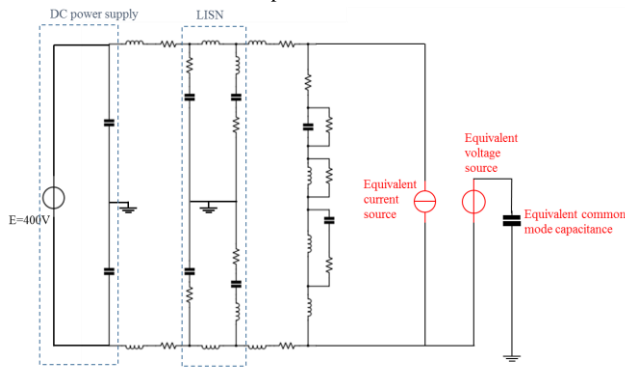


Fig. 11. Circuit with equivalent voltage and current source

into account temperature through the threshold voltage, the transconductance and the on state resistance. Thus simulations of the complete schematic of Fig. 1 were performed for different temperature and the same for the simplify schematic of Fig. 7. Comparison results are presented in Fig. 13 for two different temperatures.

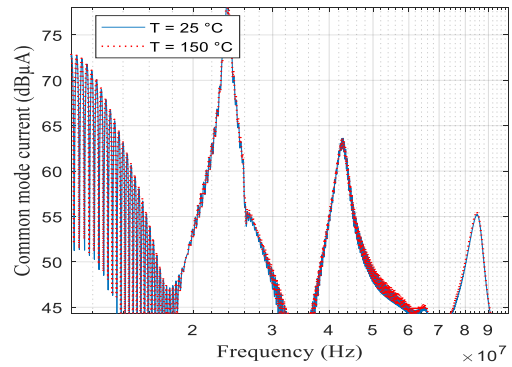


Fig. 13. Simulated spectra for different temperatures

B. Discussion

Simulation results show a slight impact of temperature on common mode spectra especially below 10 MHz. the difference appears beyond 20 MHz and is due to the variations of rising and falling time with temperature. The use of Schottky diode mitigates the recovery current which could impact the common mode spectra for high frequencies as it highly varies with temperature.

The optimization purpose requires analytical and frequency domain simulation model. The validation of the analytical waveform equations in the time domain allows the use of equivalent sources based on these equations. Transforming these equations by a Laplace transform, we can easily define frequency domain equivalent sources. All the other parts of the converter can be represented in the frequency domain by impedance matrix [6] and together with the source model, a complete EMC model can be build and use in an optimization process [7]. The so called analytical EMC model is valid up to the ten mega Hertz and is sufficient for EMC filter design.

V. CONCLUSION

This paper demonstrates the efficiency of an analytical model for EMI prediction. This model is particularly suitable for fast optimization purpose because of its derivability. It then reduce computation time and allows engineers to make multiple design test. The other important advantage of the model is its ability to predict power losses in a converter as presented in [8].

The work focus on validating the model regarding EMC problems but other works demonstrate its validity as losses estimation model and how it can be implemented in an optimization process [7].

Being able to use this analytical approach for EMC prediction and also for losses estimation considerably reduce computation time and optimization efficiency.

Acknowledgment

The authors would like to thank CORAC-Genome French National funds and Labinal Power System for their strong support.

References

- [1] T. R. McNutt, A. R. Hefner, H. A. Mantooth, D. Berning, and S. H. Ryu, "Silicon carbide power MOSFET model and parameter extraction sequence," *IEEE Trans. Power Electron.*, vol. 22, no. 2, pp. 353–363, 2007.
- [2] M. Mudholkar, M. Saadeh, and H. a. Mantooth, "A datasheet driven power MOSFET model and parameter extraction procedure for 1200V, 20A SiC MOSFETs," *Proc. 2011 14th Eur. Conf. Power Electron. Appl.*, pp. 1–10, 2011.
- [3] G. Dadanema, M. Delhommais, F. Costa, J. L. Schanen, Y. Avenas, and C. Vollaïre, "Modèle analytique d'estimation des pertes dans une cellule de commutation MOSFET-diode Schottky SiC en vue de la conception et de l'optimisation d'un dissipateur thermique," in *SGE*, 2016.
- [4] RTCA, "RTCA DO-160F. Environmental conditions and test procedures for airborne equipment," 2008.
- [5] M. Mudholkar, S. Ahmed, S. Member, M. N. Ericson, S. S. Frank, C. L. Britton, and H. A. Mantooth, "MOSFET Model," vol. 29, no. 5, pp. 2220–2228, 2014.
- [6] Bertrand Revol, "Modélisation et optimisation des performances CEM d'une association variateur de vitesse – machine asynchrone," 2003.
- [7] M. Delhommais, G. Dadanema, Y. Avenas, F. Costa, J. L. Schanen, and C. Vollaïre, "Design by Optimization of Power Electronics Converter Including EMC Constraints," in *EMC*, 2016.
- [8] G. Dadanema, F. Costa, Y. Avenas, J. L. Schanen, and C. Vollaïre, "Analytical Losses Model for SiC semiconductors dedicated to optimization operations," in *PCIM*, 2015.